THE JOURNAL OF PHYSICAL CHEMISTRY Letters

Letter

Cite This: J. Phys. Chem. Lett. 2019, 10, 5325−5330

pubs.acs.org/JPCL

Infrared Signatures of the HHe_n^+ and DHe_n^+ (n = 3−6) Complexes

Oskar Asvany,*[,†] Stephan Schlemmer,[†] Tamás Szidarovszky,[‡] and Attila G. Császár*[,‡]

[†]I. Physikalisches Institut, Universität zu Köln, Zülpicher Str. 77, 50937 Köln, Germany

[‡]Laboratory of Molecular Structure and Dynamics, Institute of Chemistry, ELTE Eötvös Loránd University and MTA-ELTE Complex Chemical Systems Research Group, Pázmány Péter sétány 1/A, H-1117 Budapest, Hungary

Supporting Information

ABSTRACT: Combination of a cryogenic ion-trap machine, operated at 4.7 K, with the free-electron-laser FELIX allows the first experimental characterization of the unusually bright antisymmetric stretch (ν_3) and π-bending (ν_2) fundamentals of the He−X^+−He (X = H, D) chromophore of the in situ prepared HHe_n^+ and DHe_n^+ (n = 3−6) complexes. The band origins obtained are fully supported by first-principles quantum-chemical computations, performed at the MP2, the CCSD(T), and occasionally the CCSDTQ levels employing extended basis sets. Both the experiments and the computations are consistent with structures for the species with n = 3 and 6 being of T-shaped C_{2v} and of D_{4h} symmetry, respectively, while the species with n = 4 are suggested to exhibit interesting dynamical phenomena related to large-amplitude motions.

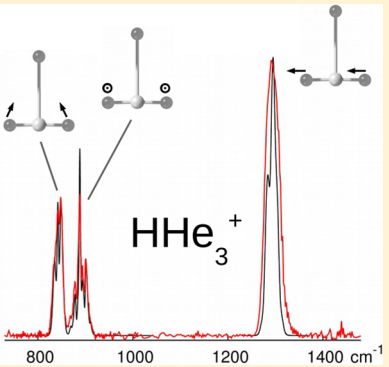

Species of the type HHe_n^+ are composed of the two most abundant elements of the universe. The first ion in this series, the strongly bound HHe^+ cation, sometimes called the hydrohelium cation, has played a decisive role in the development of the early universe.[1] It is known in the laboratory since 1925[2] and has been investigated by high-resolution vibrational[3−6] and rotational[7,8] spectroscopy. Despite a decade-long search, the detection of HHe^+ in interstellar space was achieved only very recently, via the GREAT receiver on-board the SOFIA airplane.[9]

The larger HHe_n^+ species, with $n \geq 2$, may be present in the outer atmospheres of giant gas planets and in cold plasmas. There are also speculations[10] that HHe_n^+ species with more than ∼20 solvating He atoms show the interesting quantum phenomenon of microscopic superfluidity.[11,12] Currently, these species have been investigated only by means of mass spectrometry,[2,10,13,14] revealing energetic but not structural or dynamical information. These experiments, as well as the related computations,[10] established special stabilities for complexes with "magic numbers" n = 2, 6, and 13, which seems to indicate, for example, a central role for the He−H^+−He cluster. The structures and the vibrational dynamics of this and the larger species have been elucidated by high-level first-principles quantum-chemical computations.[10,15] However, because of the rather weak interactions within the HHe_n^+ complexes, vibrational frequencies from infrared (IR) spectroscopy are needed to clarify the structure of these presumably floppy molecules.

In a more general context, proton microsolvation by noble gases received some attention, and experimental mass spectrometry,[13,16] matrix isolation spectroscopy,[17,18] and modeling[19−21] results became available. Recently, gas-phase HAr_n^+ (n = 3−7) complexes were investigated,[22] proving to be built around a strongly bound Ar−H^+−Ar core. It is an interesting question whether such a motif is also prevalent in the much weaker clusters formed with He as the noble gas. These fundamental questions on the stability, structure, and possible formation of a linear and strongly bound He−H^+−He core (the cromophore) are the motivation for this first spectroscopic investigation of the HHe_n^+ and DHe_n^+ species (n = 3−6). Because of the much weaker bond of the outer He atoms, with binding energies of not more than 200 cm^{-1},[10] four times lower than in the HAr_n^+ case,[22] we expect large-amplitude motions to be at play, posing considerable challenges to theory as well as to experiment.

The IR-active, in fact exceptionally bright,[23] antisymmetric H−He stretch (ν_3) and bend (ν_2) modes of HHe_2^+ have been predicted to be around 1350 and 890 cm^{-1}, respectively, while the predicted dissociation energy of HHe_2^+, corresponding to the $HHe_2^+ \rightarrow HHe^+ + He$ reaction, is D_0 = 4427 ± 20 cm^{-1}.[10,23] Thus, D_0 is considerably higher than the vibrational energy of these fundamentals of HHe_2^+, and it is therefore not possible to perform conventional predissociation (PD) spectroscopy on HHe_2^+ in the IR region. Because of this limitation, we focus our attention on the HHe_n^+ and DHe_n^+ complexes with $n \geq 3$, for which predissociation spectroscopy is feasible via both the ν_3 and ν_2 modes of the chromophore.

Such IRPD experiments on ionic helium complexes are best performed in cryogenic ion traps or cold jets, as demonstrated by several groups.[24−26] The central part of our setup is a 22-pole ion trapping machine called FELion.[27] In brief, HHe^+ ions

Received: July 3, 2019
Accepted: August 20, 2019
Published: August 20, 2019

DOI: 10.1021/acs.jpclett.9b01911
J. Phys. Chem. Lett. 2019, 10, 5325−5330

(similar for DHe^+) are produced in a storage ion source by electron-impact ionization of a 2:1 He−H_2 gas mixture (3:1 ratio for He−D_2). After mass selection (mass 5 u for HHe^+) in the first mass filter, an ensemble of several 10 000 ions is injected into the cold 22-pole ion trap[28] held at T = 4.7 K and stored there for typically a few seconds. An ∼100 ms He pulse at the beginning of the trapping cycle cools the ions and leads to the efficient formation of HHe_n^+ complexes up to n = 6 by ternary collisions. During the trapping time, the ionic complexes are exposed to the tunable IR pulses of FELIX.[29] After the storage and irradiation period, the ion cloud is extracted from the trap, and the complex of interest is filtered by a second mass analyzer and counted by an effective ion counter. Such storage cycles are repeated typically five times to improve the signal-to-noise ratio, after which the FELIX laser is tuned to the next frequency setting.

The FELIX laser is operated at its maximum repetition rate of 10 Hz. The laser pulse energy E is constantly monitored by a power meter at the exit of the trap machine. In the current experiment, the IR pulses are attenuated, so that the measured pulse energy is on the order of 8 mJ. The bandwidth of FELIX is transform-limited with a typical resolution of 0.2% full width at half-maximum (fwhm) of the central frequency. With this resolution, we are generally not able to resolve single rovibrational lines; only the envelopes of the vibrational bands are recovered.

For the spectroscopic investigation of the HHe_n^+ (similar for DHe_n^+) complexes, the second quadrupole mass filter is set to mass $(1 + 4n)$ u. When the FELIX frequency is on resonance, IR photodissociation occurs, for example

$$HHe_n^+ \xrightarrow{h\nu} HHe_{n-m}^+ + m\mathrm{He} \quad (n - m) \geq 2 \qquad (1)$$

which is detected as a decrease in the number of HHe_n^+ ions. The spectral signal for such measurements is obtained by counting the number of HHe_n^+ ions, $c(\tilde{\nu})$, as a function of the FELIX wavenumber $\tilde{\nu}$. The normalization procedure employed is $s(\tilde{\nu}) = (c_0 - c(\tilde{\nu}))\tilde{\nu}/(c_0 NE(\tilde{\nu}))$, with c_0 being the HHe_n^+ counts with FELIX being off-resonant, and $N \times E(\tilde{\nu})/\tilde{\nu}$ is proportional to the number of photons deposited during one trapping cycle (N shots). As all complexes with n = 1−6 are present in the trap at the same time (though with strongly decreasing number), crosstalk between the spectroscopic channels may potentially occur. We did not observe such crosstalk effects, in particular, because the distribution of HHe_n^+ complexes in every experiment was optimized via the initial He pulse.

To help understand the IRPD results, the equilibrium structures and the harmonic and the anharmonic vibrational fundamentals of all HHe_n^+ and DHe_n^+ (n = 2−6) complexes were determined at the MP2, CCSD(T), and CCSDTQ levels employing aug-cc-pVXZ basis sets with X = T, Q, and 5.[30] The anharmonic corrections to the harmonic fundamentals were determined, within second-order vibrational perturbation theory (VPT2),[31] mostly at the MP2 and CCSD(T) levels employing different basis sets (see Tables S.1 through S.4 of the Supporting Information). Apart from a few noted exceptions, the results are rather insensitive to the level of theory and the basis sets employed. The computations utilized the Gaussian16,[32] the CFOUR,[33] and the MRCC[34,35] electronic-structure codes.

In the He-solvated structures with n = 3−5, the naively expected point-group symmetry of the equilibrium structure is "lowered" by the actual geometry optimizations (see Table S.1). The equilibrium structures of HHe_3^+ and HHe_5^+ are computed to be of C_{2v} point-group symmetry, and that of HHe_4^+ is only of C_s symmetry at the highest level of theory (aug-cc-pVQZ CCSD(T)) employed. In this case, the equilibrium structure is different from a C_{2v} structure only by an exceedingly small amount. Thus, experimental data (in particular, in high resolution) are decisive to settle any dilemma about the structures and the dynamics of these ions. The equilibrium structure of HHe_6^+ has D_{4h} point-group symmetry. The calculated minimum-energy structures of the complexes, with some parameters given in Table S.1, are depicted in Figure 1.

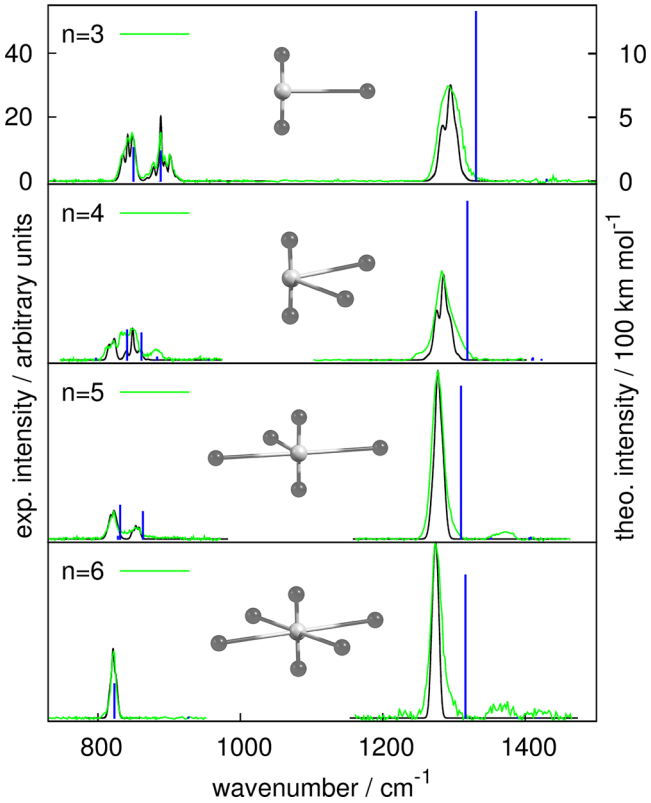

Figure 1. IR predissociation spectra of HHe_n^+, recorded in the ν_2 bending and ν_3 stretching region of the HHe_2^+ chromophore (green trace). The black lines are spectroscopic simulations with PGOPHER,[36] fitted to the measured data. The extracted band origins are given in Table 1. Blue sticks are our ab initio results from Table S.3.

For the linear molecules HHe_2^+ and DHe_2^+, the IR-allowed fundamental vibrational transitions in the targeted FELIX frequency search range are the antisymmetric stretch ν_3 and the degenerate bending ν_2, while the symmetric stretch ν_1 and the first overtones $2\nu_3$ and $2\nu_2$ are IR inactive. We confirmed the role of HHe_2^+ as being the strongly bound chromophore by attempting predissociation spectroscopy in the range of 900−1600 cm^{-1} and, as expected, did not detect any signal. For species with $n \geq 3$, however, the extra He atoms are only weakly bound,[10] and clear predissociation signals for ν_3 and ν_2 are obtained. These are summarized in Figures 1 and 2 for HHe_n^+ and DHe_n^+ (n = 3−6), respectively. For the antisymmetric stretching vibration ν_3, a slight red-shift of the band centers upon stepwise addition of He atoms is observed.

DOI: 10.1021/acs.jpclett.9b01911
J. Phys. Chem. Lett. 2019, 10, 5325−5330

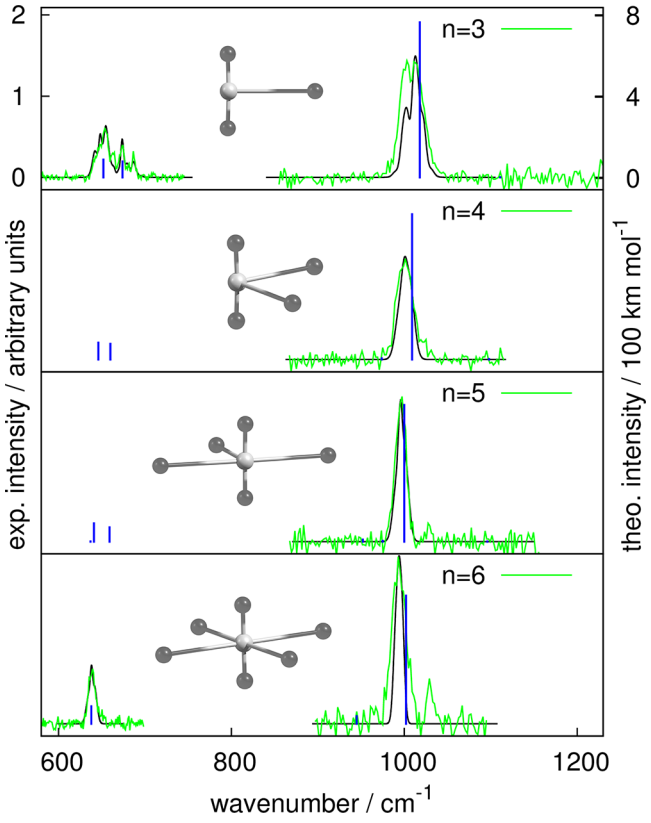

Figure 2. IR predissociation spectra of DHe_n^+, recorded in the ν_2 bending and ν_3 stretching region of the DHe_2^+ chromophore (see also caption to Figure 1). Blue sticks are our ab initio results from Table S.4.

The extracted band origins are summarized in Table 1 and compared to our anharmonic ab initio values there, as well. Also, the features for HHe_3^+ and DHe_3^+ show some structure (DHe_3^+ has, e.g., a double peak). Upon further complexation, these spectral features for ν_3 get narrower, and no obvious substructure can be seen any more.

Table 1. Experimental Band Origins (in cm^{-1}) for the Fundamental Vibrational Modes of HHe_n^+ and DHe_n^+, Extracted from Best-Fit PGOPHER Simulations to the Measured Data[a]

	ν_3		ν_2		ν_1
	expt	AI	expt	AI	AI
			HHe_n^+		
n = 2		1345		885	893
n = 3	1290	1331	841.8//887.6	850//888	886
n = 4	1282	1319	819//847	861//841	879
n = 5	1277	1310	820//853	831//863	873
n = 6	1273	1316	821	823	872
			DHe_n^+		
n = 2		1028		673	917
n = 3	1008	1018	648//673	652//674	907
n = 4	1000	1009		660//646	899
n = 5	995.5	1000		641//659	890
n = 6	993.5	1002	638	638	887

[a]These are compared to their ab initio (AI) anharmonic counterparts (see Tables S.1 and S.2 for further AI results). The experimental uncertainties of the FELIX data are typically 0.3%. The components of the "split" ν_2 fundamental are indicated as //, ordered by symmetry.

For HHe_n^+ and DHe_n^+ with n = 5 and 6, small additional features on the blue sides of the main ν_3 bands are discernible. For instance, for HHe_5^+ and HHe_6^+ these "blue bumps" are at 1372 and 1366 cm^{-1}, respectively, and thus ~95 cm^{-1} away from the main peak, while for the deuterated species there are small tentative features only ~35 cm^{-1} on the blue side of the main ν_3 peaks. These features are most probably combination bands of ν_3 with a motion of the weakly bound He atoms; similar features arising from combination bands have been observed before for other complexes, for example, for $H_3^+(H_2)_n$[37] or O_2H^+-He.[38] For HHe_6^+, we assign the observed mode to a combination of the asymmetric stretch (ν_3) with a bending motion of e_g symmetry of the four loosely bound He atoms (the harmonic and anharmonic bending fundamentals of e_g symmetry are computed to be ~170 and 100 cm^{-1}, respectively). This is the only combination band with a nonzero intensity in this region, and the anharmonic wavenumber agrees well with experiment. As to DHe_6^+, the computations indicate that the e_g-symmetry bending motion does not really depend on the mass of the central atom. Thus, the tentative feature found at an ~35 cm^{-1} shift for DHe_6^+ may not be a real feature and may be due to some experimental artifact.

As to the bending mode ν_2, the degeneracy of this mode within the chromophore HHe_2^+ is lifted in solvated HHe_n^+ complexes with n = 3–5 (similar for DHe_n^+). In our experiment, the branches of these nondegenerate modes are nicely resolved for HHe_3^+ and DHe_3^+; see Figures 1 and 2, respectively, for which one in-plane and one out-of-plane bend is discernible. For HHe_n^+ with n = 4 and 5, also two nondegenerate modes are detected, albeit with a much less resolved structure. The recording of the bending modes for the DHe_n^+ species turned out to be very challenging, due to very weak absorption dips (see the intensity discussion below) on top of a strongly varying background. Therefore, we consider the results for ν_2 of DHe_n^+ (n = 3 and 6) in Figure 2 less reliable; the spectra for n = 4 and 5 were not measured at all. For n = 6, the degeneracy is restored due to symmetry, and only a single bending mode is observed.

The intensity calibration of our measurements is reproducible within approximately a factor of 2. Therefore, the intensity variations seen in the spectra of HHe_n^+ and DHe_n^+ have to be viewed with some caution. Nevertheless, the intensity of the deuterated versions (Figure 2), being a factor of ~20 weaker compared to the hydrogenated versions (Figure 1), is striking. The significantly lower intensity could potentially be caused by isobaric contamination of the injected DHe^+ ions by D_3^+ ions and the ensuing contamination of the DHe_n^+ complexes produced. We checked that this effect is negligible by (i) minimizing the production of D_3^+ in the ion source by using a diluted 1:5 D_2/He precursor mixture and confirming the intensity shown in Figure 2, and (ii) by searching for spectral features of D_3^+–He (the degenerate stretch[39] ν_2 of D_3^+ is at 1834.67 cm^{-1}) and detecting only a tiny potential feature around 1820 cm^{-1}. The D_3^+ contamination in the injected ion ensemble is estimated to be well below 10%, and we thus conclude that the low measured intensity for the deuterated species is real. Our ab initio computations predict a weaker absorption intensity of the deuterated versions by a factor of at most 2, and it can thus be speculated that the dissociation process is causing the observed

DOI: 10.1021/acs.jpclett.9b01911
J. Phys. Chem. Lett. 2019, 10, 5325–5330

large difference between the protonated and deuterated species.

Because of the relatively high resolution of FELIX at lower wavenumbers (e.g., $\Delta\tilde{\nu} \approx 2$ cm^{-1} at $\tilde{\nu} = 800$ cm^{-1}), the rotational envelopes of the HHe_n^+ and DHe_n^+ bending modes could be resolved during our experiments, in particular, for n = 3. This made it possible to make spectroscopic simulations using the program PGOPHER;[36] see the black lines in Figures 1 and 2. In this approach, after defining the vibrational symmetries and nuclear spin weights, the spectroscopic parameters (band origins and rotational constants) are fit to the experimental observation; the best-fit band origins are given in Table 1. Concerning the nuclear spin weights, because of the zero nuclear spin (I = 0) of the He nucleus, many irreducible representations in the respective point groups of the HHe_n^+ species have zero weight (similar for DHe_n^+), and the corresponding rovibrational spectra are thus characterized by missing levels. For instance, for HHe_3^+ (C_{2v} point group) the only allowed quantum levels have symmetry A_1 and A_2, and for HHe_6^+ (D_{4h} point group) the only allowed quantum levels have symmetry A_{1g} and A_{1u}. In the PGOPHER simulations, the ab initio rotational constants (see Tables S.1 and S.2) were used as starting values (for both ground and vibrationally excited states), which, unfortunately, could not be further refined due to the low resolution of the experiments. Nevertheless, for HHe_3^+, the good agreement between measurement and simulation suggests a structure with T-shaped C_{2v} symmetry. The measurements identify the in-plane bend (a_1 symmetry, a-type) and the out-of-plane bend (b_1 symmetry, c-type) modes, with band origins at 841.8 and 887.6 cm^{-1}; see Table 1. For HHe_6^+ and DHe_6^+, the detection of one single bending mode indicates degeneracy and thus corroborates a structure of D_{4h} symmetry. For HHe_4^+, however, simulations neither in the proposed C_{2v} nor the C_s symmetries yield a satisfying fit with the measurements, indicating that large-amplitude motions of the two loosely bound He atoms may be at play. The rotational temperature in all these simulations is estimated to be ~18 K, considerably higher than the nominal trap temperature.

With similar parameters, the simulation of the measured envelopes of the antisymmetric stretch (ν_3) for HHe_n^+ and DHe_n^+ turned out to be also difficult, as the measured features are much broader than the simulated ones. In particular, the antisymmetric stretch ν_3 for HHe_3^+ (b_2 symmetry, b-type) cannot be reproduced well; for DHe_3^+ a double peak structure is observed. One can only speculate about the underlying reasons; the possibilities include perturbations, broadening of the rovibrational lines due to the short lifetime of the vibrationally excited complexes, or broadening due to saturation of the signal. High-resolution measurements are needed for clarification here, in particular, for deciphering the structure and dynamics of HHe_4^+. The band origins given in Table 1 for ν_3 are thus less accurate, but the considerable deviation from the computed results is definitely real.

This work provides the first infrared signatures for HHe_n^+ and DHe_n^+ species with $n \geq 3$. Similar to the case of the HAr_n^+ species measured by Duncan and co-workers,[22] our spectroscopic investigation clearly demonstrates experimentally that the symmetric cations He−(H/D)$^+$−He are the chromophores of these complexes. The experimental results also suggest structures for HHe_3^+ and HHe_6^+ of C_{2v} and D_{4h} point-group symmetry, respectively, by resolving the infrared bands corresponding to the bending modes of the ions. These results are clearly supported by the high-level ab initio computations of this study. The structure of HHe_4^+ and HHe_5^+ remains somewhat elusive, and more experimental work is needed to confirm the theoretical predictions, which are themselves somewhat unclear due to the polytopic nature[40−42] of these ions. It is unclear why VPT2 is unable to predict accurately the antisymmetric stretch mode (ν_3) of the HHe_n^+ and DHe_n^+ (n = 3−6) complexes (see blue sticks in Figures 1 and 2).

The chromophore itself could not be detected in this work employing the IRPD method, but the band origin of its antisymmetric stretch is now located around 1299 cm^{-1} for HHe_2^+ (1014 cm^{-1} for DHe_2^+) by simple linear extrapolation, and its π-bending mode is estimated to be at 888 cm^{-1} (673 cm^{-1} for DHe_2^+). For such an ion one can perform high-resolution rovibrational spectroscopy applying an alternative scheme, the method of state-dependent attachment of He atoms.[38,43,44] This method is based on the fact that rovibrational excitation of a cation lowers the probability of attaching loosely bound He atoms in a ternary collision process at 4 K. Experiments with high-resolution lasers at the given band positions will define the spectroscopic constants of HHe_2^+ and DHe_2^+ and their structures in all desired detail.

■ ASSOCIATED CONTENT

Supporting Information

The Supporting Information is available free of charge on the ACS Publications website at DOI: 10.1021/acs.jpclett.9b01911.

Ab initio calculations of structure, rotational constants, and vibrational frequencies of HHe_n^+ and DHe_n^+ (n = 2−6) (PDF)

■ AUTHOR INFORMATION

Corresponding Authors

*E-mail: asvany@ph1.uni-koeln.de. (O.A.)
*E-mail: csaszarag@caesar.elte.hu. (A.G.C.)

ORCID

Oskar Asvany: 0000-0003-2995-0803
Tamás Szidarovszky: 0000-0003-0878-5212
Attila G. Császár: 0000-0001-5640-191X

Notes

The authors declare no competing financial interest.

■ ACKNOWLEDGMENTS

We gratefully acknowledge the support of Radboud Univ. and of the Nederlandse Organisatie voor Wetenschappelijk Onderzoek (NWO), providing the required beam time at the FELIX Laboratory. We highly appreciate the skillful assistance of the FELIX staff. O.A. thanks S. Brünken, C. Markus, and A. N. Marimuthu for assisting in part of the FELIX shifts. The research leading to this publication has been supported by the Project CALIPSOplus under the Grant No. 730872 from the EU Framework Programme for Research and Innovation HORIZON 2020. The Hungarian coauthors are grateful to NKFIH for generous support (Grant Nos. K119658 and PD124623). This work was completed within the framework of the ELTE Excellence Program (1783-3/2018/FEKUT-STRAT) supported by the Hungarian Ministry of Human Capacities (EMMI). The German coauthors have been supported by the Deutsche Forschungsgemeinschaft (DFG) via Grant Nos. AS 319/2-2 and SCHL 341/6. Collaborative

DOI: 10.1021/acs.jpclett.9b01911
J. Phys. Chem. Lett. 2019, 10, 5325−5330

work between the Budapest and Cologne groups received support from the COST action CM1405, MOLIM: Molecules in Motion.

REFERENCES

(1) Engel, E. A.; Doss, N.; Harris, G. J.; Tennyson, J. Calculated Spectra for HeH^+ and its Effect on the Opacity of cool metal-poor Stars. *Mon. Not. R. Astron. Soc.* **2005**, *357*, 471.

(2) Hogness, T. R.; Lunn, E. G. The Ionization of Hydrogen by Electron Impact as Interpreted by positive Ray Analysis. *Phys. Rev.* **1925**, *26*, 44−55.

(3) Tolliver, D. E.; Kyrala, G. A.; Wing, W. H. Observation of the Infrared Spectrum of the Helium-Hydride Molecular Ion $^4HeH^+$. *Phys. Rev. Lett.* **1979**, *43*, 1719−1722.

(4) Bernath, P.; Amano, T. Detection of the Infrared Fundamental Band of HeH^+. *Phys. Rev. Lett.* **1982**, *48*, 20−22.

(5) Crofton, M. W.; Altman, R. S.; Haese, N. N.; Oka, T. Infrared Spectra of $^4HeH^+$, $^4HeD^+$, $^3HeH^+$, and $^3HeD^+$. *J. Chem. Phys.* **1989**, *91*, 5882−5886.

(6) Perry, A. J.; Hodges, J. N.; Markus, C. R.; Kocheril, G. S.; McCall, B. J. Communication: High Precision sub-Doppler Infrared Spectroscopy of the HeH^+ ion. *J. Chem. Phys.* **2014**, *141*, 101101.

(7) Matsushima, F.; Oka, T.; Takagi, K. Observation of the Rotational Spectra of $^4HeH^+$, $^3HeH^+$, and $^3HeD^+$. *Phys. Rev. Lett.* **1997**, *78*, 1664−1666.

(8) Liu, D.-J.; Ho, W.-C.; Oka, T. Observation of the Rotational Spectra of $^4HeH^+$, $^3HeH^+$, and $^3HeD^+$. *J. Chem. Phys.* **1987**, *87*, 2442.

(9) Güsten, R.; Wiesemeyer, H.; Neufeld, D.; Menten, K. M.; Graf, U. U.; Jacobs, K.; Klein, B.; Ricken, O.; Risacher, C.; Stutzki, J. Astrophysical Detection of the Helium Hydride Ion HeH^+. *Nature* **2019**, *568*, 357−359.

(10) Császár, A. G.; Szidarovszky, T.; Asvany, O.; Schlemmer, S. Fingerprints of Microscopic Superfluidity in HHe_n^+ Clusters. *Mol. Phys.* **2019**, *117*, 1559−1583.

(11) Grebenev, S.; Toennies, J. P.; Vilesov, A. F. Superfluidity within a Small Helium-4 Cluster: The Microscopic Andronikashvili Experiment. *Science* **1998**, *279*, 2083−2086.

(12) Toennies, J. P. Helium Clusters and Droplets: Microscopic Superfluidity and other Quantum Effects. *Mol. Phys.* **2013**, *111*, 1879−1891.

(13) Kojima, T. M.; Kobayashi, N.; Kaneko, Y. Formation of Helium Cluster Ions HH_x^+ ($x \leq 14$) and $H_3H_x^+$ ($x \leq 13$) in a very low Temperature Drift Tube. *Z. Phys. D: At., Mol. Clusters* **1992**, *23*, 181−185.

(14) Bartl, P.; Leidlmair, C.; Denifl, S.; Scheier, P.; Echt, O. Cationic Complexes of Hydrogen with Helium. *ChemPhysChem* **2013**, *14*, 227−232.

(15) Balta, B.; Gianturco, F. Structural Properties and Quantum Effects in Protonated Helium Clusters. I. The ab initio Interaction Potential. *Chem. Phys.* **2000**, *254*, 203−213.

(16) Grandinetti, F. Helium Chemistry: a Survey of the Role of the Ionic Species. *Int. J. Mass Spectrom.* **2004**, *237*, 243−267.

(17) Bondybey, V. E.; Pimentel, G. C. Infrared Absorptions of Interstitial Hydrogen Atoms in solid Argon and Krypton. *J. Chem. Phys.* **1972**, *56*, 3832−3836.

(18) Milligan, D. E.; Jacox, M. E. Infrared Spectroscopic Evidence for the Stabilization of HAr_n^+ in solid Argon at 14 K. *J. Mol. Spectrosc.* **1973**, *46*, 460−469.

(19) Beyer, M.; Lammers, A.; Savchenko, E. V.; Niedner-Schatteburg, G.; Bondybey, V. E. Proton Solvated by Noble-Gas Atoms: Simplest Case of a Solvated Ion. *Phys. Chem. Chem. Phys.* **1999**, *1*, 2213−2221.

(20) Lundell, J.; Pettersson, M.; Räsänen, M. The Proton-bound Rare Gas Compounds $(RgHRg')^+$ (Rg = Ar, Kr, Xe)—a Computational Approach. *Phys. Chem. Chem. Phys.* **1999**, *1*, 4151−4155.

(21) Baccarelli, I.; Gianturco, F. A.; Schneider, F. Spatial Structures and Electronic Excited States of small Protonated Helium Clusters. *Int. J. Quantum Chem.* **1999**, *74*, 193.

(22) McDonald, D. C.; Mauney, D. T.; Leicht, D.; Marks, J. H.; Tan, J. A.; Kuo, J.-L.; Duncan, M. A. Communication: Trapping a Proton in Argon: Spectroscopy and Theory of the Proton-bound Argon Dimer and its Solvation. *J. Chem. Phys.* **2016**, *145*, 231101.

(23) Stephan, C. J.; Fortenberry, R. C. The Interstellar Formation and Spectra of the Noble Gas, Proton-Bound $HeHHe^+$, $HeHNe^+$ and $HeHAr^+$ Complexes. *Mon. Not. R. Astron. Soc.* **2017**, *469*, 339−346.

(24) Bieske, E.; Dopfer, O. High Resolution Spectroscopy of Ionic Complexes. *Chem. Rev.* **2000**, *100*, 3963−3998.

(25) Brümmer, M.; Kaposta, C.; Santambrogio, G.; Asmis, K. R. Formation and Photodepletion of Cluster Ion-Messenger Atom Complexes in a Cold Ion Trap: Infrared Spectroscopy of VO^+, VO_2^+, and VO_3^+. *J. Chem. Phys.* **2003**, *119*, 12700−12703.

(26) Jašík, J.; Žabka, J.; Roithová, J.; Gerlich, D. Infrared Spectroscopy of Trapped Molecular Dications below 4 K. *Int. J. Mass Spectrom.* **2013**, *354*, 204−210.

(27) Jusko, P.; Brünken, S.; Asvany, O.; Thorwirth, S.; Stoffels, A.; van der Meer, L.; Berden, G.; Redlich, B.; Oomens, J.; Schlemmer, S. The FELion Cryogenic Ion Trap Beam Line at the FELIX Free-Electron Laser Laboratory: Infrared Signatures of Primary Alcohol Cations. *Faraday Discuss.* **2019**, *217*, 172−202.

(28) Asvany, O.; Bielau, F.; Moratschke, D.; Krause, J.; Schlemmer, S. New Design of a Cryogenic Linear RF Multipole Trap. *Rev. Sci. Instrum.* **2010**, *81*, 076102.

(29) Oepts, D.; van der Meer, A. F. G.; van Amersfoort, P. W. The Free-Electron-Laser User Facility FELIX. *Infrared Phys. Technol.* **1995**, *36*, 297−308.

(30) Dunning, T. H., Jr. Gaussian Basis Sets for Use in Correlated Molecular Calculations. *J. Chem. Phys.* **1989**, *90*, 1007−1023.

(31) Bloino, J.; Biczysko, M.; Barone, V. General Perturbative Approach for Spectroscopy, Thermodynamics and Kinetics: Methodological Background and Benchmark Studies. *J. Chem. Theory Comput.* **2012**, *8*, 1015−1036.

(32) Frisch, M. J.; et al. *Gaussian16 Revision B.01;* Gaussian, Inc.: Wallingford, CT, 2016.

(33) For the current version, see http://www.cfour.de. For detailed contributions from authors, see ref 2 in the Supporting Information.

(34) Rolik, Z.; Szegedy, L.; Ladjánszki, I.; Ladóczki, B.; Kállay, M. An Efficient Linear-Scaling CCSD(T) Method Based on Local Natural Orbitals. *J. Chem. Phys.* **2013**, *139*, 094105.

(35) For the current version of the MRCC code, see http://www.mrcc.hu.

(36) Western, C. M. PGOPHER: A Program for Simulating Rotational, Vibrational and Electronic Spectra. *J. Quant. Spectrosc. Radiat. Transfer* **2017**, *186*, 221−242.

(37) Okumura, M.; Yeh, L. I.; Lee, Y. T. The Vibrational Predissociation Spectroscopy of Hydrogen Cluster Ions. *J. Chem. Phys.* **1985**, *83*, 3705−3706.

(38) Kohguchi, H.; Jusko, P.; Yamada, K. M. T.; Schlemmer, S.; Asvany, O. High-Resolution Infrared Spectroscopy of O_2H^+ in a Cryogenic Ion Trap. *J. Chem. Phys.* **2018**, *148*, 144303.

(39) Amano, T.; Chan, M.-C.; Civis, S.; McKellar, A. R. W.; Majewski, W. A.; Sadovskii, D.; Watson, J. K. G. The Infrared Vibration-Rotation Spectrum of the D_3^+ Molecular Ion: Extension to higher Vibrational and Rotational Quantum Numbers. *Can. J. Phys.* **1994**, *72*, 1007−1015.

(40) Clementi, E.; Kistenmacher, H.; Popkie, H. Study of the Electronic Structure of Molecules. XVIII. Interaction between a Lithium Atom and a Cyano Group as an Example of a Polytopic Bond. *J. Chem. Phys.* **1973**, *58*, 2460−2466.

(41) Nielsen, I. M. B.; Allen, W. D.; Császár, A. G.; Schaefer, H. F. Toward Resolution of the Silicon Dicarbide (SiC_2) Saga: *Ab initio* Excursions in the Web of Polytopism. *J. Chem. Phys.* **1997**, *107*, 1195−1211.

(42) Császár, A. G.; Allen, W. D.; Schaefer, H. F., III In Pursuit of the ab initio Limit for Conformational Energy Prototypes. *J. Chem. Phys.* **1998**, *108*, 9751−9764.

DOI: 10.1021/acs.jpclett.9b01911
J. Phys. Chem. Lett. 2019, 10, 5325−5330

(43) Asvany, O.; Brünken, S.; Kluge, L.; Schlemmer, S. COLTRAP: a 22-pole Ion Trapping Machine for Spectroscopy at 4 K. *Appl. Phys. B: Lasers Opt.* **2014**, *114*, 203−211.
(44) Doménech, J. L.; Jusko, P.; Schlemmer, S.; Asvany, O. The First Laboratory Detection of Vibration-Rotation Transitions of $^{12}CH^+$ and $^{13}CH^+$ and Improved Measurement of their Rotational Transition Frequencies. *Astrophys. J.* **2018**, *857*, 61.

DOI: 10.1021/acs.jpclett.9b01911
J. Phys. Chem. Lett. 2019, 10, 5325−5330